

RESEARCH

Open Access



Complement activity and autophagy are dysregulated in the lungs of patients with nonresolvable COVID-19 requiring lung transplantation

Pooja Shivshankar^{1,2,3*†}, Stacey L. Mueller-Ortiz^{2†}, Aleksey Y. Domozhrov², Weizhen Bi¹, Scott D. Collum¹, Marie-Francoise Doursout⁴, Manish Patel⁵, Isabella N. LeFebvre⁵, Bindu Akkanti⁶, Simon Yau⁷, Howard J. Huang⁷, Rahat Hussain⁵ and Harry Karmouty-Quintana^{1,6*}

Abstract

The severe acute respiratory syndrome coronavirus 2 (SARS-CoV-2)-induced coronavirus disease 2019 (COVID-19) pandemic has challenged the current understanding of the complement cascade mechanisms of host immune responses during infection-induced nonresolvable lung disease. While the complement system is involved in opsonization and phagocytosis of the invading pathogens, uncontrolled complement activation also leads to aberrant autophagic response and tissue damage. Our recent study revealed unique pathologic and fibrotic signature genes associated with epithelial bronchiolization in the lung tissues of patients with nonresolvable COVID-19 (NR-COVID-19) requiring lung transplantation. However, there is a knowledge gap if complement components are modulated to contribute to tissue damage and the fibrotic phenotype during NR-COVID-19. We, therefore, aimed to study the role of the complement factors and their corresponding regulatory proteins in the pathogenesis of NR-COVID-19. We further examined the association of complement components with mediators of the host autophagic response. We observed significant upregulation of the expression of the classical pathway factor *C1qrs* and alternative complement factors *C3* and *C5a*, as well as the anaphylatoxin receptor *C5aR1*, in NR-COVID-19 lung tissues. Of note, complement regulatory protein, decay accelerating factor (DAF; *CD55*) was significantly downregulated at both transcript and protein levels in the NR-COVID-19 lungs, indicating a dampened host protective response. Furthermore, we observed significantly decreased levels of the autophagy mediators PPAR γ and LC3a/b, which was corroborated by decreased expression of *factor P* and the C3b receptor *CR1*, indicating impaired clearance of damaged cells that may contribute to the fibrotic phenotype in NR-COVID-19 patients. Thus, our study revealed previously unrecognized complement dysregulation associated with impaired cell death and clearance of damaged cells, which may promote NR-COVID-19 in patients, ultimately necessitating lung transplantation. The identified network

[†]Pooja Shivshankar and Stacey L. Mueller-Ortiz have contributed equally to this work.

*Correspondence:

Pooja Shivshankar
Pooja.Shivshankar@uth.tmc.edu
Harry Karmouty-Quintana
Harry.Karmouty@uth.tmc.edu

Full list of author information is available at the end of the article



© The Author(s) 2025. **Open Access** This article is licensed under a Creative Commons Attribution-NonCommercial-NoDerivatives 4.0 International License, which permits any non-commercial use, sharing, distribution and reproduction in any medium or format, as long as you give appropriate credit to the original author(s) and the source, provide a link to the Creative Commons licence, and indicate if you modified the licensed material. You do not have permission under this licence to share adapted material derived from this article or parts of it. The images or other third party material in this article are included in the article's Creative Commons licence, unless indicated otherwise in a credit line to the material. If material is not included in the article's Creative Commons licence and your intended use is not permitted by statutory regulation or exceeds the permitted use, you will need to obtain permission directly from the copyright holder. To view a copy of this licence, visit <http://creativecommons.org/licenses/by-nc-nd/4.0/>.

of dysregulated complement cascade activity indicates the interplay of regulatory factors and the receptor-mediated modulation of host immune and autophagic responses as potential therapeutic targets for treating NR-COVID-19.

Keywords Nonresolvable COVID-19, Pulmonary fibrosis, Complement-mediated immunity, Complement activation, Autophagy, C3a and C5a anaphylatoxins, Receptor signaling

Introduction

Virulent human coronaviruses, such as severe acute respiratory syndrome coronavirus (SARS-CoV), which emerged in 2003, Middle East respiratory syndrome coronavirus (MERS-CoV), and the recently emerged SARS-CoV-2 [1], bind to ACE2 receptors on airway and lung epithelial cells and alveolar resident macrophages [2]. COVID-19 pathogenesis primarily affects lung function via acute respiratory distress syndrome (ARDS) and pneumonia, along with diffuse alveolar damage (DAD). Alveolar macrophage-driven endothelial loss, thrombus formation, and cytokine storms evolve into life-threatening hypoxia [3]. The inflammatory and hypoxic state is followed by the development of mucus plugs with fibrinous exudates, resulting in severe COVID-19 in an age-independent manner and multiple organ dysfunction in some patients [4, 5]. The fibroproliferative phenotype of type II pneumocytes is the next stage that determines epithelial cell fate and regeneration and results in “non-resolvable” clinical conditions in patients, thereby requiring ventilation and necessitating lung transplantation [6, 7]. We recently demonstrated that nonresolvable COVID-19 (NR-COVID-19) lungs significantly express the extracellular matrix proteins periostin (POSTN) and collagen 1 and 3 components (COL1A2 and COL3A1), along with the profibrotic mediator alpha-smooth muscle actin (α -SMA) collagen triple helix-repeat containing 1 (CTHRC1). The fibrotic phenotype also involves high levels of keratin 8 expression, indicating a transitional state of alveolar epithelial cells with basal cells expressing keratin 5, resulting in alveolar bronchiolization. These fibrotic phenotypes demonstrated sustained myofibroblast activation and fulminant lung fibrosis within an average of 119 days (ranging from 55–211 days) of contracting the infection, thereby requiring lung transplantation [8].

However, the heterogeneity of the host immune response observed in respiratory failure patients might lead to unresolved pathologic outcomes in NR-COVID-19 patients, that is, patients requiring lung transplantation. For example, lung autopsies from patients with high viral burdens, including deceased COVID-19 patients, demonstrated increased interferon-gamma (IFN γ) responses and enrichment of inflammatory macrophage (M1) phenotypes. Moreover, a low viral burden is correlated with patient-specific inflammatory

signatures, mucin production, and expression of surfactant-producing genes [9]. The levels of circulatory complement anaphylatoxins C3a and C5a, upon alternative complement pathway activation, are significantly elevated in different stages of COVID-19, including pneumonia, ARDS, and critical illness, and are positively correlated with in-hospital mortality, not survival [10, 11]. In MERS-CoV-infected individuals, increased *C3a* and *C5a* transcript levels in the lungs are also positively correlated with disease severity [12]. In addition, C3 hydrolysis and increased levels of the positive regulatory factors D and P are also correlated with increased disease severity and increased mortality in SARS-CoV-2- and MERS-CoV-infected individuals [12, 13]. However, the role of the complement system in modulating lung tissue inflammation and pathology in end-stage NR-COVID-19 is not clearly understood.

The complement system, comprising more than 30 soluble and surface-bound proteins, lies at the interface of innate and adaptive immune responses in both acute infectious and chronic inflammatory diseases [14–16]. C1q, in the classical complement pathway, serves as an immune checkpoint and triggers complement activation when viral antigens bind to IgM, rapidly appearing within 3–7 days post-infection [17, 18]. A recent study linked IgM glycosylation and increased C1q and C3 deposition with disease severity in COVID-19 patients [19]. Increased C3 levels are also a potential mechanism of pulmonary fibrosis with uncontrolled complement activation in idiopathic pulmonary fibrosis patients with gain-of-function polymorphisms in the mucin 5B gene *MUC5B* [20]. While genetic predisposition to SARS-CoV infection in individuals was associated with C-type lectin gene polymorphisms [21–23], lectin receptors with conserved SARS-CoV-2 glycosylation binding sites were also identified to activate lectin complement pathway signaling [24]. Respiratory failure in SARS-CoV-2-infected individuals was associated with increased MAC (C5b-C9), complement component C4D, and MBL-associated serine protease *MASP2* expression with DAD in lung autopsies, and similar activation was observed in purpuric skin lesions in these patients [25]. In a recent study, the SARS-CoV-2-N protein was shown to directly bind *MASP2* on the cell surface, resulting in lectin pathway overactivation [26].

As a surveillance mechanism, complement immune factors activate the autophagic response in damaged or microbially infected cells through signaling via damage-associated molecular patterns (DAMPs) and pathogen-associated molecular patterns (PAMPs) [27]. Clusterin is a human apolipoprotein that sequesters circulating C7 and other MAC components (C5b-9) and renders it inactive [28, 29]. Clusterin also facilitates the lipidation of the autophagy mediator LC3 and induces mitophagy via the coordinated function of PPARgamma (PPAR γ) [30, 31]. PPAR γ activity is also negatively correlated with the levels of complement factors, including C3, C5, and C7 [32]. Interestingly, preclinical studies have shown that alveolar macrophage PPAR γ suppresses influenza virus-induced long-term fibrotic sequelae. Together, these studies highlight the inverse correlation of the levels of complement factors with autophagy-mediated cell survival mechanisms, which we aimed to investigate in NR-COVID-19 lungs.

During viral pathogenesis, soluble regulatory complement factor H and surface-bound regulatory factors, including CD46, CD55, and CD59, are exploited by viruses to prevent infection-induced cell neutralization and destruction, thereby increasing alternative complement pathway activation via factor B and factor P activity, leading to tissue destruction [33, 34]. In addition, both viral and bacterial molecular patterns interact with CD46, which is sometimes referred to as a “pathogen magnet”, and could be linked to xenophagy, the autophagic defense against intracellular pathogens possibly triggered by microbial effectors [35–38]. Paradoxically, viral infections could benefit from the autophagic response to virion packaging by utilizing the small membranous vesicles formed during autophagic degradation [39, 40].

Hence, in this study, we sought to determine whether complement immune cascade activities are altered during the progression of lung fibrosis in NR-COVID-19 patients and whether the membrane-bound or soluble regulatory factors of the complement system are affected in NR-COVID-19-related fibrosis. Further analysis of the expression levels of the C3a and C5a anaphylatoxin receptors showed significantly increased C5aR1 levels, indicating its role in inflammatory signaling in NR-COVID-19 patients. Finally, we observed that the levels of autophagic mediators PPAR γ and LC3a/b were significantly downregulated in the NR-COVID-19 lung tissues. Taken together, these findings suggested that activated complement factors may potentially block PPAR γ / LC3a/b -mediated autophagic rescue mechanisms in the end stage of the NR-COVID-19.

Materials and methods

Human lung specimens

The use of human lung explants in this study was approved by the internal review boards of the University of Texas Health Science Center at Houston (HSC-MS-15-1049 and HSC-MS-08-0354), Houston Methodist Hospital (Pro00003392), and Baylor College of Medicine (H-46823) and were performed in adherence to the Declaration of Helsinki. Lung explants from patients with NR-COVID-19 (designated COVID#) were processed within one hour of the lung transplantation procedure. Similarly, this study used discarded lung transplant donor tissues from LifeGift Organ Procurement (Houston, TX) as controls (designated Cont#). All tissues were collected from the middle regions of the upper and lower lobes as detailed previously [8, 41]. The excised tissues were stored in the ice box and transported within one hour. The collection and storage of the tissue explants were performed at the UTHealth Center of Pulmonary Excellence (UTHealth-PCOE) for research studies. Table 1 shows the patients’ age, sex, and ethnicity. The patients in the control cohort (41.5 ± 14.1 years old) were age-matched with NR-COVID-19 patients (46.0 ± 15.0 years old). Signed informed consent was obtained from all patients for the research study (Clinical trial number: not applicable).

RNA isolation and quantitative RT–PCR assay

Human lung explants were pulverized in liquid nitrogen, and the powder was stored in liquid nitrogen until further use. RNA isolation from the frozen pulverized tissues was carried out via Qiagen miniprep columns following the manufacturer’s protocol, and the samples were DNase-treated via ArcticZymes Kits. The RNA concentrations were measured using NanoDrop 2000 Spectrophotometer (Thermo Scientific; Cat# ND-2000C), and 1 μ g of the extracted total RNA was reverse transcribed using a High-Capacity cDNA Reverse Transcription Kit (Applied Biosystems; Waltham, MA). The resulting

Table 1 Tissue sample demographic information

	Control	NR-COVID-19
Age (Years \pm SD)	41.5 \pm 14.1	46.0 \pm 15.0
Female sex	3/12	2/12
Male sex	9/12	10/12
Ethnic group	B:1 C:8 H:3	B:0 C:4 H:8
BMI (AU \pm SD)	26.3 \pm 3.1	25.6 \pm 2.2
N number	12	12

The table shows the demographic information of the human discarded tissues used in this study

B Black, C Caucasian, H Hispanic

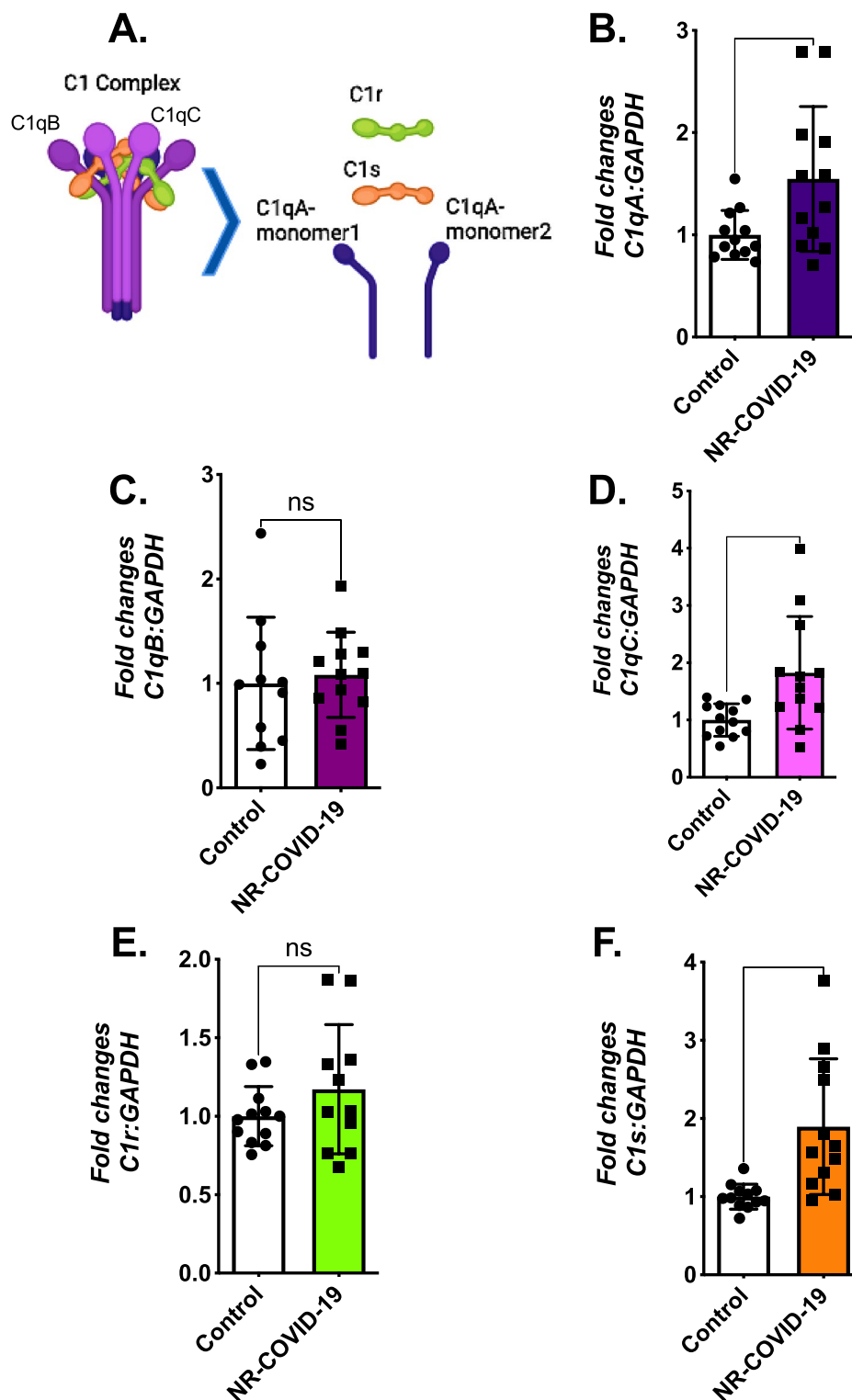


Fig. 1 The lungs of patients with NR-COVID-19 exhibit altered expression of the classical complement factors *C1q* and *C1s*. **A** The schematic depicts the complement 1 (*C1*) complex. The *C1* complex is made up of dimers of three *C1q* subunits, *C1qA* (blue), *C1qB* (magenta), and *C1qC* (pink), and dimers of the serine proteases *C1r* (green) and *C1s* (orange). The bar graphs show the mRNA levels of **B** *C1qA*, **C** *C1qB*, **D** *C1qC*, **E** *C1r*, and **F** *C1s* measured via RT-qPCR in lung RNA extracts. The values represented in the bar graphs are the means \pm SEs of the fold change in expression in lung explants from NR-COVID-19 patients normalized to that in control lungs (control expression set to 1.00). The expression levels in both cohorts were normalized to those of the internal housekeeping gene *GAPDH*. Statistical significance was determined at the level of * $P < 0.05$; *** $P < 0.001$ (N = 12 for each cohort)

cDNA was stored at -20°C until use. Three microliters of the 1:10-diluted cDNA was subjected to quantitative PCR (qPCR) assays using specific primers for each tested transcript and iTaq Universal SYBR Green Supermix (Bio-Rad, Hercules, CA). The delta CT values (ΔCT) (test vs. housekeeping gene *GAPDH*) for each amplicon were normalized to those of the control tissues ($\Delta\Delta\text{CT}$), and the expression levels were designated as the fold change in expression using Bio-Rad CFX Maestro™ Software in the lungs of NR-COVID-19 patients compared with those in control lungs. QuantiTect™ primers from Qiagen (Germantown, MD) were used for the qPCR assays and are listed in Supplemental Table 1.

Western blotting

Total protein from the frozen lung tissue powders was extracted via the use of Invitrogen radioimmunoprecipitation assay buffer supplemented with Halt™ protease and phosphatase inhibitor cocktail (Thermo Fisher, Waltham, MA). Protein concentrations were measured using bicinchoninic acid (BCA) reagent (Pierce), and 30 μg of total protein was subjected to electrophoretic separation with Bio-Rad gradient gels (4–12%). The separated proteins were transferred onto a PVDF membrane, and immunoblotting for complement proteins was carried out using specific antibodies. Supplemental Table 2 details the antibody specifications and dilutions used in the study. The blots were developed with a West Q Pico-ECL solution (GenDepot, Baker, TX), and the intensity of each band was quantified from the acquired images via Bio-Rad Image Lab 6.1 software. The data are presented as ratios of the band intensities of the test proteins to those of the housekeeping proteins β -actin, GAPDH, or β -tubulin as loading controls. Suitable housekeeping proteins were chosen based on our previous experiments demonstrating transfer efficiency and consistent expression across groups [8].

Statistical analyses

Statistical analyses were carried out using GraphPad Prism 9.3. A two-tailed unpaired *t*-test with Welch's correction was performed to determine statistical significance. The outliers were identified via the ROUT method, which employs a false discovery rate with non-linear regression to remove multiple outliers [42]. Differences in transcript and protein expression levels at a *P* value < 0.05 were considered statistically significant.

Results

Classical complement and lectin pathway factors are differentially expressed in NR-COVID-19 lungs

First, to determine the presence of the classical pathway components of C1qrs in NR-COVID-19 lungs, we investigated the mRNA levels of *C1q.r.s* in control and NR-COVID-19 lung tissues (Fig. 1). The expression of classical complement C1qrs factors is critical for the initial activation of the complement cascade by pathogen recognition and antigen–antibody interactions (schematic; Fig. 1A). The *C1q.r.s* (C1qrs) subunits are expressed independently from different genetic loci. While the three subunits *C1qA*, *B*, and *C* are encoded by chromosome 1, the C1r and C1s subunits are encoded by chromosome 12 [43–45]. Therefore, we measured individual transcript levels in both control and NR-COVID-19 lung tissues. We observed a 1.5-fold increase in *C1qA* expression ($p = 0.024$; Fig. 1B) and a 1.8-fold increase in *C1qC* expression ($p = 0.015$; Fig. 1D) in the lungs of NR-COVID-19 patients compared with those in the lungs of control patients. *C1qB* expression was not significantly different between the groups (Fig. 1C). Although *C1r* mRNA levels were not significantly different (Fig. 1E), *C1s* mRNA levels were significantly increased by 1.9-fold in the lungs of NR-COVID-19 patients compared with those in control lungs ($p = 0.004$; Fig. 1F). Together, NR-COVID-19 lungs presented differential expression of *C1*

(See figure on next page.)

Fig. 2 The lungs of patients with NR-COVID-19 show upregulation of the complement factors C3 and C4. **A** A schematic representation of three distinct complement pathways is shown here. The classical pathway is activated by antigen (from pathogens or self-antigens) and antibody (IgM and IgG) interactions. Once hexameric C1q binds to the antigen–antibody complex, the activated C1s cleaves C4 and C2 into C4a and C4b and C2a and C2b, respectively. C4a and C2b bind to form classical C3 convertase (C2aC4b), leading to the cleavage of C3 into C3a and C3b. The lectin pathway independently activates C3 convertase (C2aC4b) via MBL-associated serine proteases (MASP-1 and MASP-2) that cleave C2 and C4, leading to the formation of C3a and C3b. The alternative complement pathway is activated during infections and chronic inflammatory conditions through spontaneous hydrolysis of C3, giving rise to alternative C3b, which binds factor D to cleave factor B into Bb. C3b and Bb binding leads to the generation of alternative C3 (C3bBb) and C5 convertases (C3bBbC3b), which initiate an activation loop for the uncontrolled generation of C3a and C5a anaphylatoxins. The C5b fragments further participate in activating membrane attack complex (MAC, C5b-C9) formation. Regulatory C4-binding proteins (C4bp: 2 subunits, C4bpA and C4bpB) inhibit the lectin pathway and C3 convertase activity to mitigate the generation of C3a and C5a anaphylatoxins and MAC formation. The bar graphs show the mRNA levels of **B** C2, **C** C3, **D** C4a, **E** C4b, **F** C4bpA, and **G** C4bpB measured via RT-qPCR in lung RNA extracts. The values represented in the bar graphs are the means \pm SEs of the fold change in expression in lung explants from NR-COVID-19 patients normalized to that in control lungs (control expression set to 1.00). The expression levels in both cohorts were normalized to those of the internal housekeeping gene *GAPDH*. Statistical significance was determined at the level of * $P < 0.05$; *** $P < 0.001$ ($n = 12$ for each cohort)

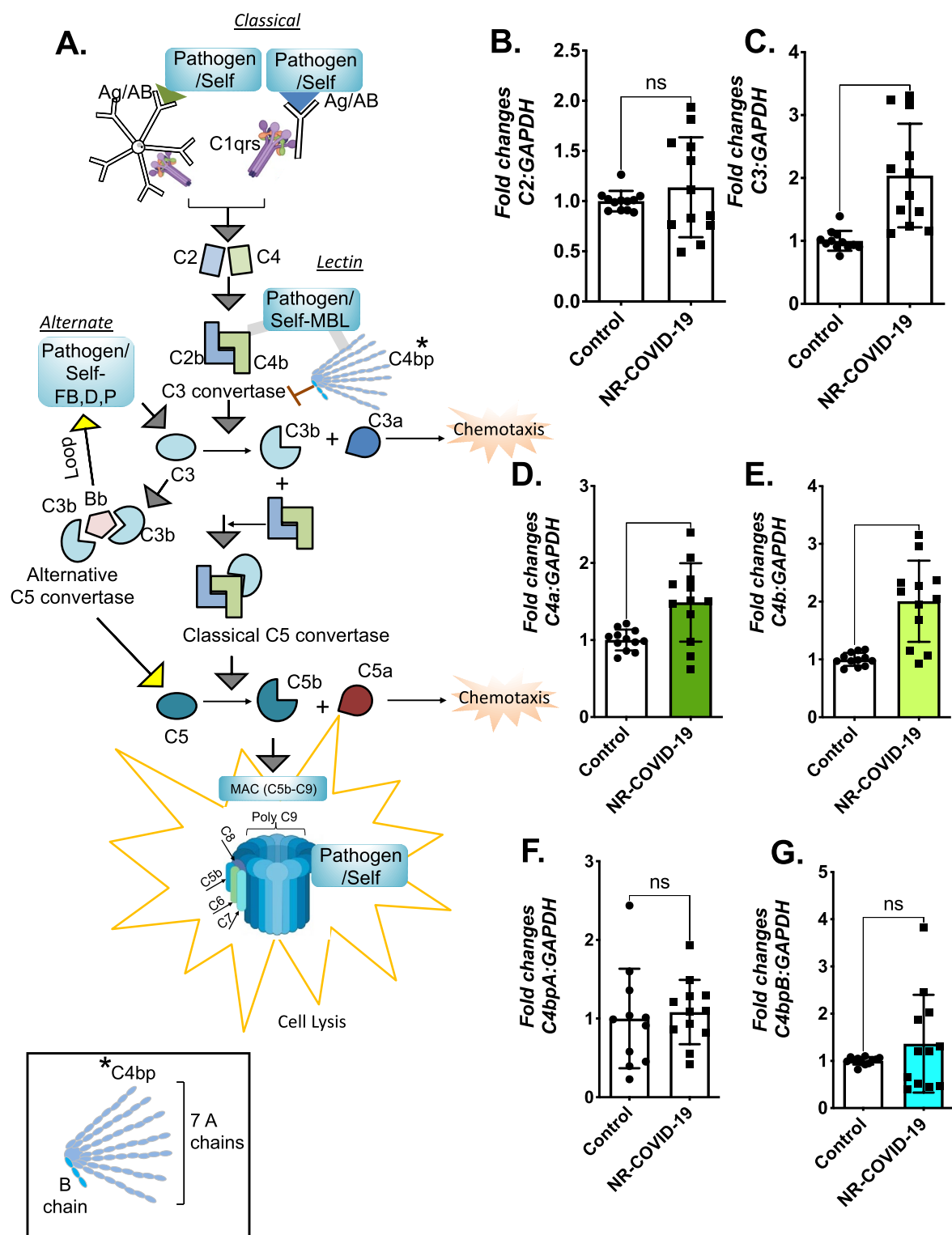


Fig. 2 (See legend on previous page.)

components, suggesting an abnormal classical pathway response in end-stage disease.

We further analyzed the transcript levels of the downstream complement factors C2, C3, and C4, which are subsequently activated by classical C1 and lectin pathway

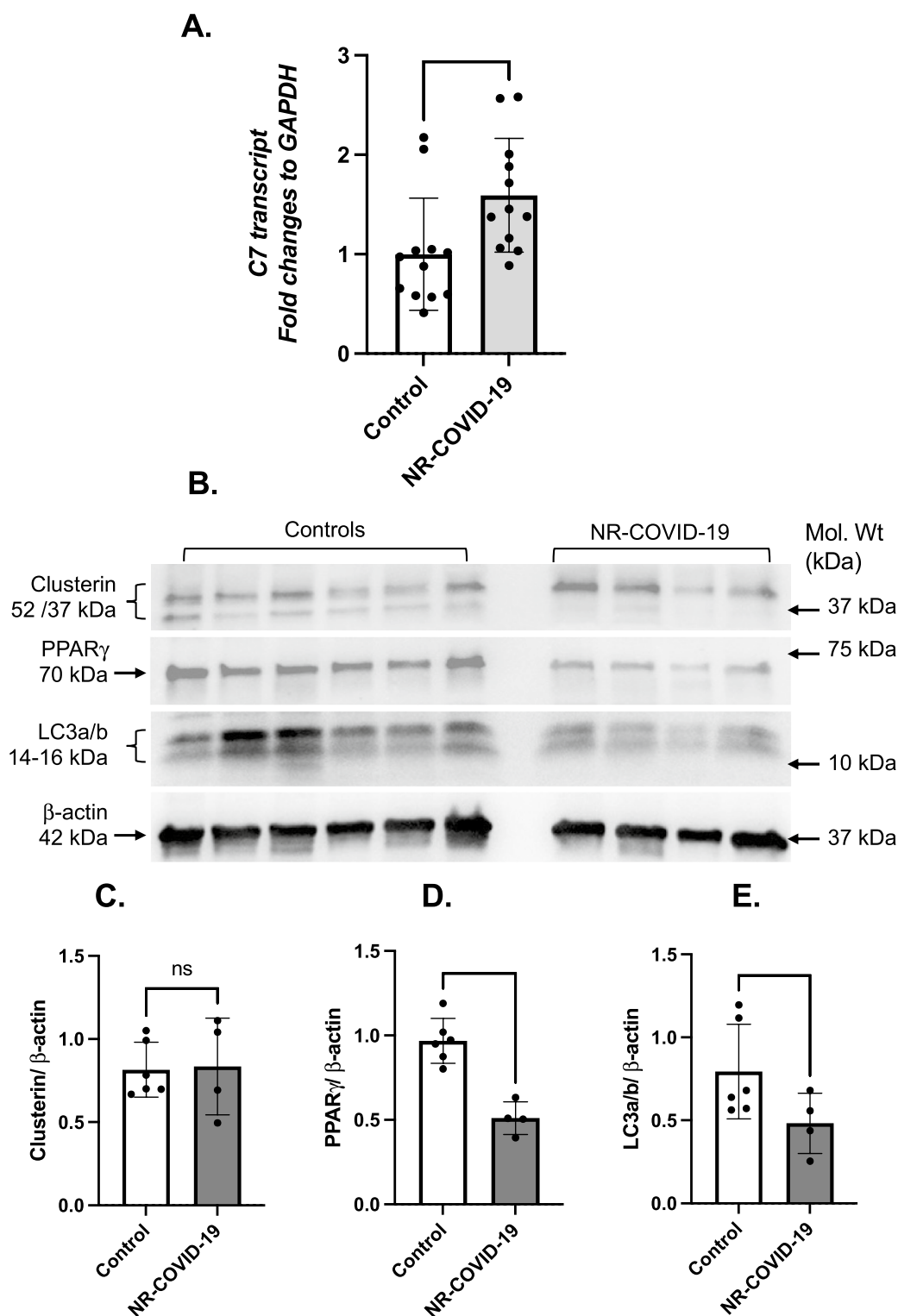


Fig. 3 Expression of C7 autophagy markers in the lungs of NR-COVID-19 patients. **A** The bar graphs show the mRNA levels of C7, which were measured via RT-qPCR assays, in control lung tissues and lung tissues from NR-COVID-19 patients. The values are presented as the means \pm SEs of the fold change in expression in the lung explants from NR-COVID-19 patients normalized to that in the control lungs (control expression levels set to 1.00). **B** Representative western blots showing the protein levels of clusterin, PPAR γ , and LC3a/b along with the loading control β -actin in control lung homogenates and lung homogenates from NR-COVID-19 patients. The bar graphs shown below represent the mean densitometric quantification as arbitrary ratios of the protein levels to those in the loading control. Statistical significance was determined at the level of * $P < 0.05$; *** $P < 0.001$ (N=6 for control; N=4 for NR-COVID-19)

components (schematic; Fig. 2A). Although C2 mRNA levels were not significantly different between the groups (Fig. 2B), C3 mRNA levels were considerably greater (2.0-fold; $p=0.0011$; Fig. 2C) in the lungs of NR-COVID-19 patients than in those of control patients. Furthermore, we measured complement C4 expression via primers specific for *C4a* and *C4b*, since these genes are expressed independently, and the proteins complex to form the full-length C4 protein [46]. We observed a 1.5-fold increase in *C4a* expression ($p=0.007$; Fig. 2D) and a 2.0-fold increase in *C4b* expression ($p=0.0004$; Fig. 2E) in the lungs of NR-COVID-19 patients compared with those in control samples. Interestingly, the expression levels of the regulatory C4-binding protein (C4BP) subunits, *C4bpA* and *C4bpB* (Fig. 2F and G), did not differ between the groups. Furthermore, we observed significant upregulation of *MASP2* mRNA to 2.6-fold in NR-COVID-19 lungs ($p=0.0009$; Supplemental Fig. 1). Together, the data revealed that the upregulation of C3, *C4a*, and *C4b* transcripts may be due to aberrant activation of the upstream C1 and MBL complexes in NR-COVID-19 lungs.

Complement factor 7 and host autophagy pathway components in NR-COVID-19

To determine the expression of complement factors and complement-associated autophagic mediators, we investigated the expression levels of MAC components (C5b-C9) and autophagy markers. Interestingly, we observed a significant increase in C7 transcript levels in the lungs of NR-COVID-19 patients (Fig. 3A). However, the mRNA levels of the MAC components C5, C6, and C8b were not significantly different between the groups (Supplemental Fig. 2). Transcripts for C8a and C9 were not detectable in the lung tissue from either group. The upregulation of C7 mRNA expression may independently contribute to dysregulated inflammatory and apoptotic mechanisms leading to lung fibrosis in NR-COVID-19 patients [47, 48]. To understand the MAC sequestering effect of clusterin in NR-COVID-19 patients, we measured the protein levels of clusterin in control lungs (N=6) and the lungs of

NR-COVID-19 patients (N=4). We observed no significant difference in clusterin levels between the two groups (Fig. 3B, C). These findings suggest vascular/endothelial-mediated local C7 expression [48, 49]. Clusterin is also important for the biogenesis of autophagosome formation via LC3 lipidation. It also acts as a molecular chaperone along with PPAR γ in modulating PPAR γ levels and the LC3 lipidation facilitator clusterin [30], a human apolipoprotein that sequesters the effects of circulating complement factor C7 and other membrane attack complex components (MAC; C5b-9), resulting in an inactive complex.

Furthermore, the levels of the autophagy markers PPAR γ (Fig. 3B, D) and LC3a/b (Fig. 3B, E) were significantly decreased in the lungs of NR-COVID-19 patients. Furthermore, we investigated candidates for the complement-driven antimicrobial innate autophagic response [37], namely, ATG7 and ULK-1 (Supplemental Fig. 3). We found a decreasing trend in the transcript levels of these genes in NR-COVID-19 lungs compared with those in control lungs (Supplemental Fig. 3). Together with unaltered clusterin levels, these data suggest that the autophagic response is also inhibited in NR-COVID-19, which may contribute to defective resolution, enhanced immunopathology, and fibrosis [29, 50, 51].

Differential expression of anaphylatoxin receptors in NR-COVID-19 lung explants

The complement anaphylatoxins C3a and C5a are generated from the cleavage of their respective precursors C3 and C5 and serve as proinflammatory mediators by binding to their respective receptors C3aR and C5aR1 and the decoy receptor of C5a, C5aR2, to promote chemotaxis and induce immune cell activation (schematic; Fig. 4A) [52–54]. C3a and C5a are further cleaved by carboxypeptidase M (CPM), resulting in more stable but less active forms of C3a and C5a known as C3a_{desArg} and C5a_{desArg} [55]. In the NR-COVID-19 lung explants, we observed significant upregulation of *C3aR* mRNA

(See figure on next page.)

Fig. 4 The expression of the C3a and C5a anaphylatoxin receptors in the lungs of NR-COVID-19 patients. **A** Schematic showing how the C3a and C5a anaphylatoxin receptors C3aR, C5aR1 and C5aR2 interact at the cell membrane. The membrane-bound carboxypeptidase M regulates anaphylatoxin receptor-mediated signaling by cleaving the carboxy-terminal arginine from C3a and C5a, resulting in the formation of less active C3a_{desArg} and C5a_{desArg}. The bar graphs show the mRNA levels of **B** *C3aR*, **C** *C5aR1*, **D** *C5aR2*, and **E** *CPM*, which were measured via RT-qPCR in lung RNA extracts. The values represented in the bar graphs are the means \pm SEs of the fold change in expression in lung explants from NR-COVID-19 patients normalized to that in control lungs (control expression set to 1.00; (N = 12 per group)). The expression levels in both cohorts were normalized to those of the internal housekeeping gene *GAPDH*. Statistical significance was determined at the level of $P < 0.05$ ($n = 12$ for each cohort). **F** Representative immunoblots showing the protein levels of C3aR, C5aR1, C5aR2, and CPM in control lung tissues and lung tissues from NR-COVID-19 patients. The bar graphs (**G–J**) represent the mean densitometric quantification data given as arbitrary ratios of the intensity of bands for receptors to that of their respective loading controls (N=6 for each cohort; in the C5aR1 blot, sample 5 ratio in the control group was omitted as an outlier measured by the ROUT method (Q = 1%). Statistical significance was determined at the level of $*P < 0.05$; $***P < 0.001$

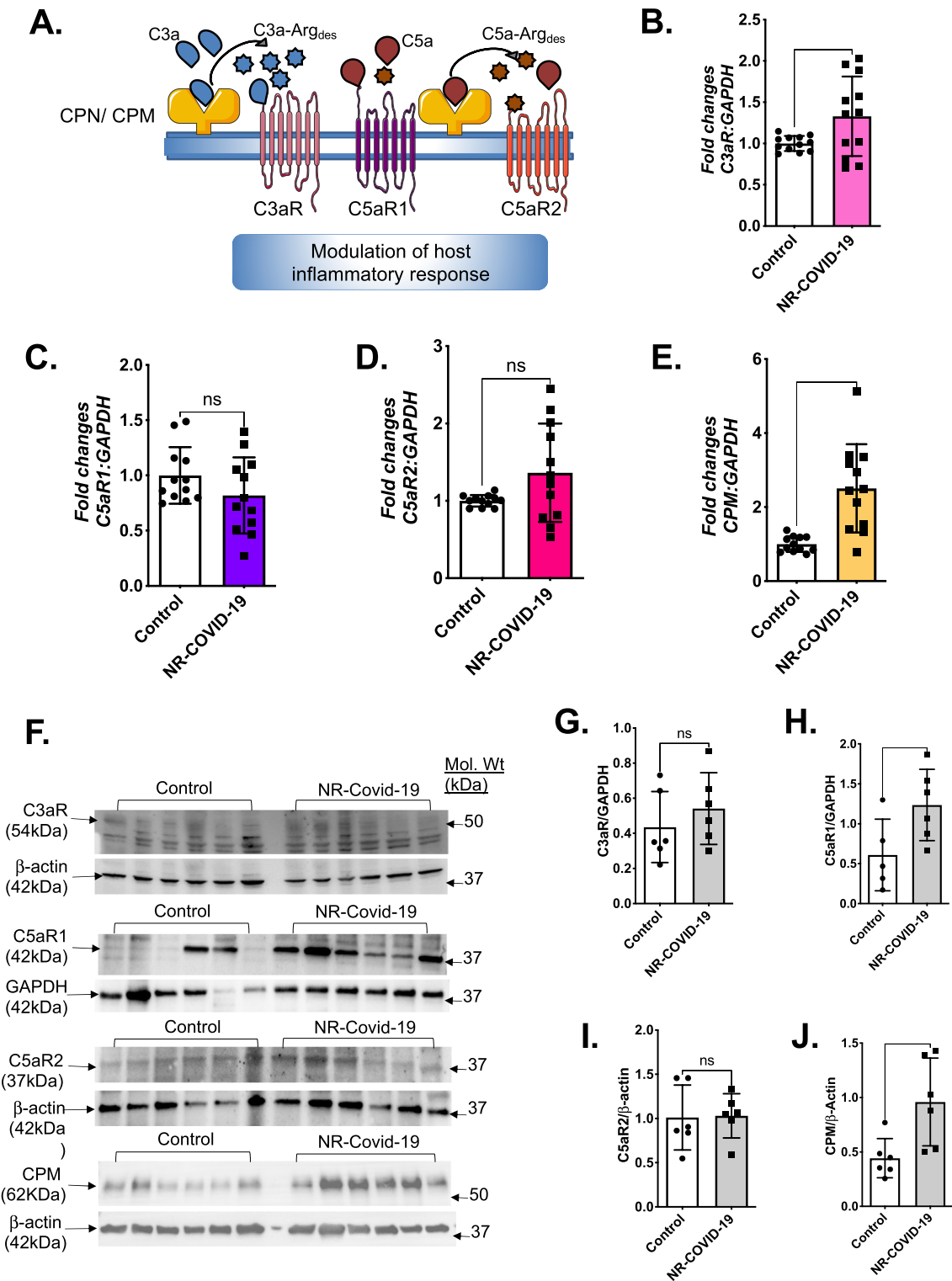


Fig. 4 (See legend on previous page.)

expression (Fig. 4B). However, *C5aR1* and *C5aR2* (Fig. 4C and D) mRNA levels did not significantly differ between the lungs of NR-COVID-19 patients and control patients.

On the other hand, we observed significant upregulation of *CPM* mRNA levels in the lungs of NR-COVID-19 patients (Fig. 4E). As shown by representative western

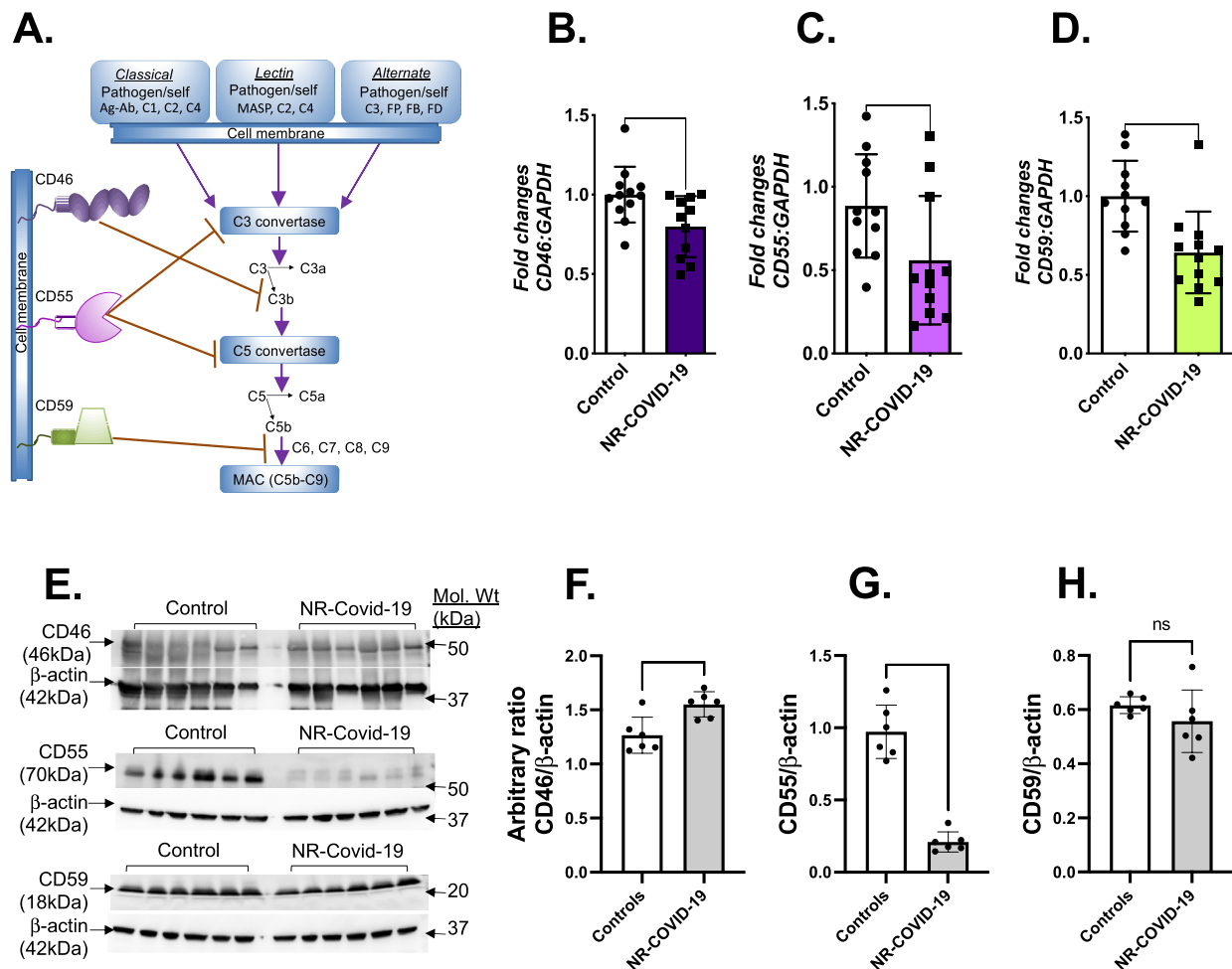


Fig. 5 The expression of the membrane-bound regulatory proteins CD46, CD55, and CD59 is downregulated in the lungs of patients with NR-COVID-19. **A** Schematic representation of the membrane-bound regulatory proteins CD46, CD55, and CD59 that regulate C3 and C5 convertase activity and MAC formation. The soluble factor I coactivates CD46 activity to prevent C3b from forming C5 convertase. The bar graphs show the mRNA levels of **B** CD46, **C** CD55, and **D** CD59, which were measured via RT-QPCR in lung RNA extracts. The values represented in the bar graphs are the means \pm SEs of the fold change in expression in nrCOVID-19-PF lung explants normalized to that in control lungs (control expression set to 1.00; N = 12 for each cohort). The expression levels in both cohorts were normalized to those of the internal housekeeping gene GAPDH. **E** Representative immunoblots showing the protein levels of CD46, CD55, and CD59 along with the loading control β -actin in control lung tissues and lung tissues from NR-COVID-19 patients. The bar graphs (**F–H**) represent the mean densitometric quantification data given as arbitrary ratios of the intensity of bands for receptors to that of their respective loading controls (N = 6 per group). Statistical significance was determined at the level of * $P < 0.05$; *** $P < 0.001$.

blots, we observed no significant difference in the protein levels of C3aR (Fig. 4F and G), of the two C5a binding receptors, C5aR1 protein levels were significantly elevated in the lungs of NR-COVID-19 patients (Fig. 4F and H). Consistent with the mRNA levels, there was no significant difference in the protein levels of the decoy receptor C5aR2 (Fig. 4F and I). These results indicate the discrepancy of synchrony between the mRNA and protein levels due to differential host responses [56–59], particularly with overabundant transcriptional enrichment as observed in severe COVID-19 [58]. Finally, CPM

protein levels were significantly greater in NR-COVID-19 lungs than in control lungs (Fig. 4F and J). These results indicate a positive correlation of C5aR1 levels with increased CPM production as a host response in C5a cleavage and mitigation of C5aR1 signaling.

The membrane-bound regulatory factors of the complement system are differentially expressed in NR-COVID-19 lungs

We further assessed the expression levels of the membrane-bound regulatory factors CD46, CD55, and

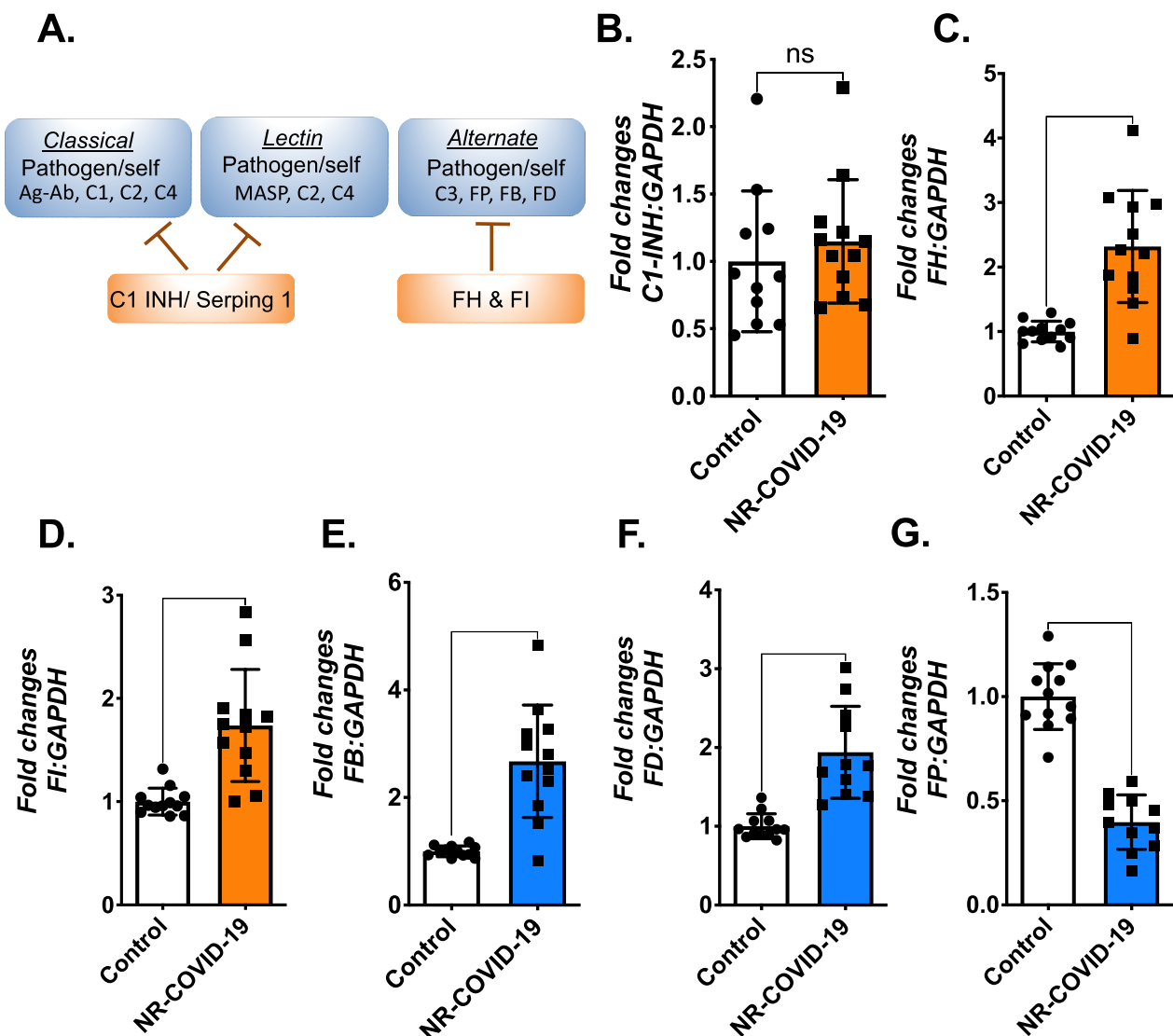


Fig. 6 The expression of soluble regulatory factors is downregulated in the lungs of NR-COVID-19 patients. **A** Schematic representation of how soluble regulatory proteins function in all three complement pathways. The negative regulator C1-INH (also called SerpinG1) inhibits C1s cleavage of C2 and C4, thereby restricting the formation of the C3 convertase. Factor H and Factor I inhibit the alternative complement pathway from establishing an amplification loop. Factor P stabilizes the binding of C3b to the cell surface to induce pathogen phagocytosis and damage cell apoptosis. The bar graphs show the mRNA levels of the negative regulators **B** C1-INH, **C** FH, and **D** FI and the transcript levels of the soluble positive regulators **E** FB, **F** FD, and **G** FP, as measured via RT-qPCR assays of lung RNA extracts. The values represented in the bar graphs are the means \pm SEs of the fold change in expression in lung explants from NR-COVID-19 patients normalized to that in control lungs (control expression set to 1.00). The expression levels in both cohorts were normalized to those of the internal housekeeping gene *GAPDH*. Statistical significance was determined at the level of * $P < 0.05$; *** $P < 0.001$ ($N = 12$ for each cohort)

CD59 (schematic; Fig. 5A), which may be involved in mitigating tissue damage caused by pathologic complement activation during NR-COVID-19-induced lung fibrosis. To our surprise, the levels of CD46, CD55, and CD59 expression were significantly lower (Fig. 5B–D) in the lungs of NR-COVID-19 patients than in those of control patients, which could lead to overactivation of the complement system and potential

cell damage and tissue injury. However, the protein levels of these membrane-bound receptors demonstrated a distinct pattern of protein levels. While CD46 protein levels were significantly increased in the lungs of NR-COVID-19 patients, we observed a significant decrease in the CD55 protein levels concordant with the mRNA levels, and the CD59 protein levels remained unchanged (Fig. 4E–H). These data suggest

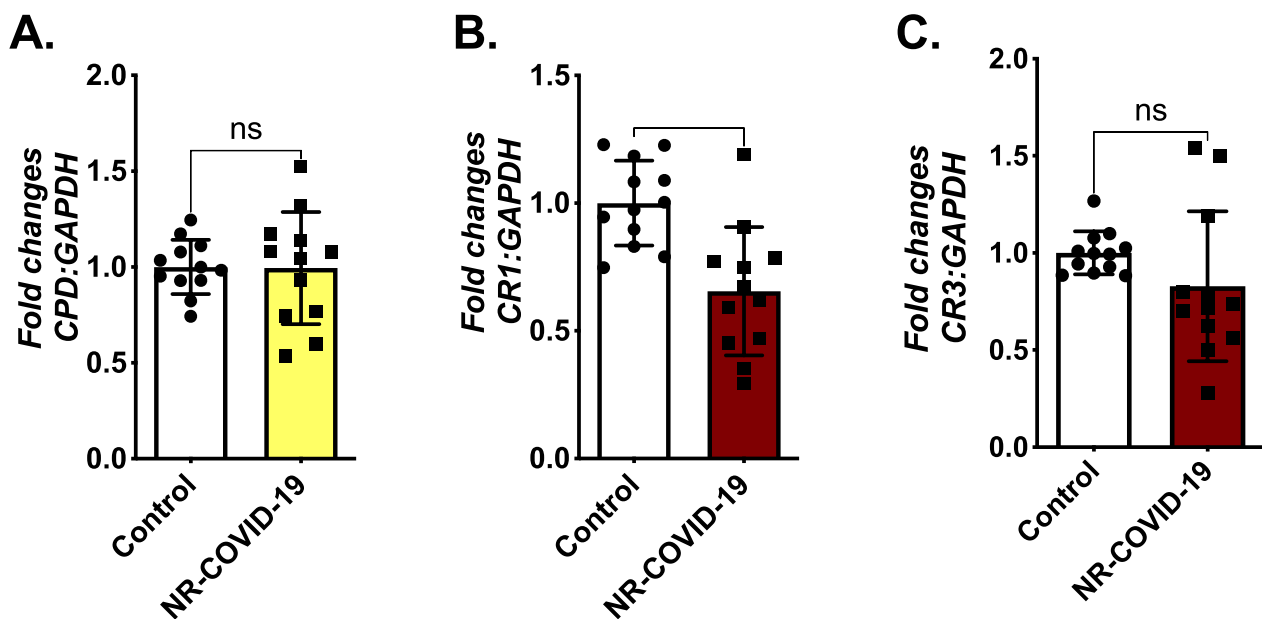


Fig. 7 Expression levels of immune cell receptors in the lungs of NR-COVID-19 patients. The bar graph shows the mRNA levels of **A** CPD, **B** CR1, and **C** CR3, which were measured via RT-qPCR via lung RNA extracts. The values represented in the bar graphs are the means \pm SEs of the fold change in expression in lung explants from NR-COVID-19 patients normalized to that in control lungs (control expression set to 1.00). The expression levels in both cohorts were normalized to those of the internal housekeeping gene *GAPDH*. Statistical significance was determined at the level of $*P < 0.05$; $***P < 0.001$ ($N = 12$ for each cohort)

a lack of strong correlation between mRNA and protein levels due to cellular stress-induced inflammatory mechanisms and overwhelmed inflammatory response, particularly in severe COVID-19 disease [56–60].

Soluble regulatory factors of the complement system are differentially expressed in NR-COVID-19 lungs

Regarding soluble complement regulatory proteins, as depicted in the schematic (Fig. 6A), the negative soluble regulator C1-INH (also known as SerpinG1) inhibits both the classical and lectin pathways. FH and FI inhibit the alternative complement pathway. We assessed the expression levels of these negative regulators in the lung tissues of controls and NR-COVID-19 patients. While the transcript levels of *C1-INH* were similar between the groups (Fig. 6B), both *FH* and *FI* mRNA levels were significantly greater in the lungs of NR-COVID-19 patients than in those of control patients (Fig. 6C and D). On the other hand, positive regulators of the alternative complement pathway, *FB* and *FD*, were also significantly upregulated in the lungs of NR-COVID-19 patients (Fig. 6E and F), indicating that the amplification loop of C3 cleavage by spontaneous hydrolysis or direct pathogen binding is activated in the lungs of NR-COVID-19 patients. In contrast, the expression of *FP*, which is involved in stabilizing C3 convertase, was significantly downregulated in the

lungs of NR-COVID-19 patients (Fig. 6G). These findings indicate that the host response controls alternative pathway activation.

The expression of the immune cell-specific complement regulatory protein CR1 is downregulated in the lungs of NR-COVID-19 patients

Immune cell-specific carboxypeptidase D cleaves the C-terminal arginine in peptides and proteins and is highly expressed in LPS-exposed macrophages [61, 62]. CR1 and CR3 are both C3b-binding receptors expressed on immune cells and are involved in the apoptotic clearance of damaged cells [63]. Among the three tested immune cell-specific complement regulators in the lungs of NR-COVID-19 patients (Fig. 7A–C), the expression of *CR1* (also known as *CD35*) was significantly downregulated (Fig. 7B). However, the expression of CPD and the other immune cell receptor *CR3* was not altered in the lungs of NR-COVID-19 patients. CR1 expression in the erythrocytes is also decreased in COVID-19 ICU patients. It is associated with inhibitory complement factor I, consistent with our observation of significantly upregulated FI mRNA in the lungs of NR-COVID-19 patients (Fig. 6D) [64]. Together with decreased levels of *FP* mRNA, a significant decrease in CR1 expression indicates delayed apoptotic clearance of damaged cells during the progression of end-stage NR-COVID-19.

Discussion

In this investigation, we report significant dysregulation of complement immune factors in the lungs of NR-COVID-19 patients compared with those in the lungs of the control cohort. We analyzed the mRNA and protein levels of complement factors and the associated autophagic response in uncontrolled complement activation-induced tissue damage in nonresolving COVID-19 lung disease. The complement system is an important component of immunity and is activated by damaged cells and pathogenic stimuli. By examining the transcript levels of the components of all three cascades and the regulators of complement activation, we identified the interplay of these factors in the progression to the non-resolving disease stage in COVID-19 patients. Regarding the classical complement pathway, increased expression of *C1qA*, *C1qC*, and *C1s* mRNAs in NR-COVID-19 lungs suggests independent functionality of C1q and C1s without complexing with the C1r subunits [65–67]. Increased levels of *C1q* subunits also indicate the complement-independent effects of C1q on its non-IgG ligand C-reactive protein (CRP), the level of which is highly elevated in COVID-19 patients [68, 69]. Moreover, C1q can directly bind to pathogen surfaces and initiate a host humoral response and the formation of a C3 convertase, resulting in anaphylatoxin release and a heightened inflammatory response [16, 33, 70]. Thus, we observed independent and sustained activation of classical complement factors until the end stage of NR-COVID-19.

Increased mRNA levels of the lectin pathway component MASP2 indicate the coordinated activity of C1s and MASP2 in activating downstream effectors, the formation of C3 convertases, and subsequent alternative complement activation [71–76]. Plasma MASP2 concentrations are also significantly elevated in COVID-19 patients and are associated with downstream complement activation [77]. The lectin pathway is regulated by C4BP, which inhibits MASP-2-mediated cleavage of C4 and the generation of the active peptides C4a and C4b [78]. In our study, significantly increased mRNA levels of *C4a* and *C4b* in NR-COVID-19 lungs indicate the potential involvement of sustained classical and lectin pathway activation in the progression of lung fibrosis in NR-COVID-19 patients.

The mRNA levels of the central complement factor for all three cascades, C3, were significantly increased in the lungs of NR-COVID-19 patients. This increased C3 message level suggests the involvement of C3 in the tissue injury and fibrosis observed in the lungs of NR-COVID-19 patients, as observed in IPF patients with mucus hypersecretions [20]. The C3-derived ligand C3b binds to the CR1/CD35 receptor on B cells, thereby inducing humoral and cell-mediated/adaptive immune

responses to control viral infectivity and protect the lungs against viral propagation [79–81]. To our surprise, we observed a significant reduction in CR1/CD35 gene expression in the lungs of NR-COVID-19 patients, suggesting potentially dampened humoral and cell-mediated immune responses. The upregulation of *C3aR* mRNA and C5aR1 protein levels observed in the lungs may further contribute to the proinflammatory state and sustained tissue damage [11]. Therefore, the pathologic complement-mediated inflammation and tissue damage could involve C3, FB, C3aR, and C5aR1. A recent in vitro study on SARS-CoV-2-infected airway epithelial cells revealed that neutralization of C5aR1 suppressed inflammation and maintained epithelial integrity [82]. Although they noted upregulation of C5aR2, we did not find any significant changes in the mRNA or protein levels of C5aR2. Since C5aR2 has a greater affinity for C5a_{desArg} [82], our data suggest that the full-length C5a/C5aR1 signaling axis may be involved in the progression of NR-COVID-19.

Autophagy is generally considered a homeostatic response that involves the recycling of subcellular organelles instead of complete apoptosis. An inefficient autophagic response is evident in both autoimmune diseases and infectious diseases [83–85]. Influenza viral infection has been shown to down-regulate PPAR γ function, thereby inducing lung injury [51]. We observed that the levels of the autophagy markers PPAR γ and LC3a/b were significantly decreased in the lungs of NR-COVID-19 patients. While clusterin facilitates the autophagic response via LC3a/b, our data revealed unaltered clusterin levels, with significant decreases in LC3a/b and PPAR γ levels in the lungs of NR-COVID-19 patients, thereby contributing to defective resolution and fibrosis [29, 30, 50, 51, 86]. Although complement factor C7 is a component of the MAC, it is also expressed as a membrane protein in endothelial cells [48]. Importantly, endothelial C7 acts as a trap for the assembling terminal complex and mediates anti-inflammatory effects by inhibiting endothelial IL8 production and decreasing the levels of surface adhesion molecules, therefore preventing immune cell infiltration and vascular leakage [49]. Given that clusterin also sequesters circulating MAC components [28], the absence of C8 and C9 transcripts of the MAC components and unchanged clusterin levels suggest that local C7 expression may be contributed by inflamed endothelial cells in the lungs of patients with NR-COVID-19. C7 is also expressed in the stromal cells of both human and mouse prostate and has been shown to suppress prostate cancer growth by inducing cellular apoptosis [47]. These studies support our explanation that the pulmonary vasculature and stroma might contribute to lung tissue expression of C7 during the severity

of COVID-19 and that apoptotic mechanisms might trigger end-stage fibrosis.

We further observed that alternative complement pathway activation during lung fibrosis in NR-COVID-19 patients was accompanied by the downregulation of membrane-bound regulatory factors, such as *CD46*, *CD55*, and *CD59* messages, which are involved in the apoptotic clearance of damaged cells. Similar downregulation of *CD55* and *CD59* has been observed in herpes virus infection [87]. Moreover, full-length and the variant forms BC1, BC2, C1, and C2 of *CD46* serve as membrane receptors for viruses and bacterial binding [88–90], which could possibly explain the increased *CD46* protein levels in NR-COVID-19 lungs. In agreement with the mRNA levels, we observed a significant decrease in *CD55* (DAF) protein levels in NR-COVID-19 lungs, suggesting a dampened regulatory response during the pathogenesis of NR-COVID-19. A recent study has demonstrated SARS-CoV2 hijacking of DAF and *CD59* as a potential immune escape mechanism to block complement-mediated virolysis [91]. Because the DAF inhibits C3 and C5 convertase activity and inhibits alternative complement activation, a decrease in DAF may be associated with uncontrolled complement activation in NR-COVID-19. Treatment with C5 neutralizing antibody, *pezelimab*, in DAF deficiency-associated conditions such as angiothrombotic thrombocytopenic purpura, inhibited complement hyperactivation [92]. Interestingly, histological findings of lung autopsies of COVID-19 patients have shown increased protein levels of all three regulatory proteins [93]. The authors correlated increased C3 production as the inflammatory consequence and the upregulated regulatory proteins as the host protective response.

In the case of soluble factors, *FP* contributes to the alternative complement pathway by stabilizing alternative C3 convertases [94]. A complement-independent role has been demonstrated for properdin in binding to pathogens. *FP* deficiency is also associated with sustained tissue damage [38, 95, 96], as we have observed significantly reduced *FP* expression levels in lung tissues in NR-COVID-19 patients. In contrast, we observed significant upregulation of *FB* and *FD* expression in these NR-COVID-19 tissues compared with those in the controls, indicating uncontrolled alternative pathway activation. Significantly elevated serum levels of factor B and its byproducts were measured in COVID-19 patients admitted to the intensive care unit, and *FD* levels were elevated significantly in deceased patients compared with those who survived, suggesting the potential roles of these positive regulators in sustained amplification of the alternative complement pathway, resulting in exacerbated inflammation and ARDS [97]. Furthermore, the complement-inhibiting factor *FH* blocks the formation

of the alternative complement pathway C3 convertase, and *FI* interacts with various proteins, including *FH*, to inhibit the C3 convertase activities of both the classical (C2aC4b) and alternative (C3bBb) pathways, in addition to directly binding to pathogenic viruses [98–100]. The increased expression levels of these soluble regulatory factors in NR-COVID-19 lungs may indicate a sustained host antiviral and anti-inflammatory response.

Finally, our results revealed that the pathogenesis of NR-COVID-19 involves the activation and maintenance of the alternative complement pathway and potentially reduces the apoptotic clearance of damaged cells via a reduction in the expression of *CR1/CD35* and *FP*. Efferocytosis is the process of apoptotic cell clearance. The initial phase of COVID-19-related ARDS, comprising neutrophil infiltration with a cytokine storm, is in part promoted by alternative complement pathway signaling, following which *CR3* (C3b-binding receptor; a dimer of *CD11b* and *CD18*) induces phagocytosis of damaged/apoptotic neutrophils by macrophages [101]. However, the lungs of NR-COVID-19 patients expressed lower levels of *CR3*, suggesting that an impaired efferocytosis mechanism may contribute to the NR-COVID-19-related fibrotic phenotype [101]. Thus, our data collectively suggest that the persistence of alternative complement activation with increased C3 production, together with impaired efferocytosis, may lead to the development of NR-COVID-19 in patients, ultimately requiring lung transplantation. Taken together, our data suggest that in addition to aberrant complement activation and impaired regulatory factor functionality, dysregulation of autophagy and its severity may contribute to NR-COVID-19 lung disease.

Concluding remarks

In this study, we analyzed complement activation in NR-COVID-19 lungs and its association with the aberrant host autophagic response. Although there are a few limitations in this study, including the availability of samples, it is the first study, to our knowledge, to comprehensively elucidate the local presence of the components of the three pathways and regulators of complement activation (RCAs). We are also the first to investigate the involvement of autophagic mediators as a potential mechanism underlying dysregulated complement-induced tissue damage leading to end-stage respiratory failure. Anti-C5a antibodies, including *vilobelimab*, have been studied in phase 2 and phase 3 clinical case studies in invasively ventilated COVID-19 patients [102, 103] to address the consequences of acute and sustained complement. Although neutralization of C5a with *vilobelimab* improved the survival rate

by 32% for all-cause mortality rate, compared with 42% in placebo-treated patients at 28 days, serious treatment-emergent adverse events (TEAE) was observed in 59% of patients, versus 63% in individuals that received the placebo [102]. Clinical intervention with the anti-C5aR1 antibody avdoralimab did not significantly improve the clinical outcome of COVID-19-related ARDS patients (clinical trial # NCT04371367) [104]. Thus, our findings suggest that instead of blocking the activity of alternative complement factors and their receptor-mediated signaling, restoring the impaired functions of the membrane-bound regulatory protein, CD55, and CD59 and the immune-specific receptors CR1/CR3 to increase the phagocytic clearance of damaged cells and to restore the autophagic response and mitigate pathologic progression evident in the lungs of patients with NR-COVID-19, preventing the need for lung transplantation, is more beneficial.

Supplementary Information

The online version contains supplementary material available at <https://doi.org/10.1186/s12931-025-03152-6>.

Supplementary Material 1. Supplemental Fig. 1. The bar graphs show the mRNA levels of *MASP2*, which were measured via RT-qPCR in control lung tissues and lung tissues from NR-COVID-19 patients. The values represent the mean \pm SE of the fold change in expression in lung explants from NR-COVID-19 patients normalized to that in control lungs (control expression set to 1.00). The expression levels in both cohorts were normalized to those of the internal housekeeping gene *GAPDH*. Statistical significance was determined at the level of $*P < 0.05$; $***P < 0.001$ ($N = 12$ for each cohort). Supplemental Fig. 2. A Schematic showing the MAC complex containing C5b, C6, C7, C8 and polymeric C9. The bar graphs show the mRNA levels of B C5, C C6, and D C8b, which were measured via RT-qPCR in lung RNA extracts. The values represented in the bar graphs are the means \pm SEs of the fold change in expression in lung explants from NR-COVID-19 patients normalized to that in control lungs (control expression set to 1.00). The expression levels in both cohorts were normalized to those of the internal housekeeping gene *GAPDH*. Statistical significance was determined at the levels of $*P < 0.05$ and $***P < 0.001$ ($N = 12$ for each cohort). Supplemental Fig. 3. The bar graphs show the mRNA levels of *ATG7* and *ULK-1* in lung tissue extracts from NR-COVID-19 patients and controls, which were measured via RT-QPCR. The values represented in the bar graphs are the means \pm SEs of the fold change in expression in lung explants from NR-COVID-19 patients normalized to that in control lungs (control expression set to 1.00). The expression levels in both cohorts were normalized to those of the internal housekeeping gene *18S*. Statistical significance was determined at the level of $*P < 0.05$; $***P < 0.001$ ($N = 12$ for each cohort).

Supplementary Material 2.

Acknowledgements

Nature publishing author services for scientific editing of the manuscript

Author contributions

PS designed the study, acquired the data, analyzed and interpreted the results, prepared the figures and drafted the manuscript. SLM-O, AYD, WB, SDC acquired the data, analyzed and interpreted the results. MFD, BA, analyzed and interpreted the results. INLF, SY, HJH provided key material, analyzed and interpreted clinical data. HKQ designed the study, analyzed and interpreted the results, and drafted the manuscript. All authors read and approved the final manuscript.

Funding

This work was also supported by NIH funding to PS (R01 AI158694-01) and an NIH-CTSA pilot award (5UL1TR003167-05).

Availability of data and materials

No datasets were generated or analysed during the current study.

Declarations

Ethics approval and consent to participate

Study protocols for analyzing deidentified human specimens were approved and waiver of consent was granted by the Institutional Review Board of UTHealth Houston Committee for Protection of Human Subjects and research was performed in accordance to the Declaration of Helsinki.

Consent for publication

Not applicable.

Competing interests

The authors declare no competing interests.

Author details

¹Department of Biochemistry and Molecular Biology, University of Texas Health Science Center at Houston, Houston, TX, USA. ²Hans J. Müller-Eberhard and Irma Gigli Center for Immunology and Autoimmune Diseases, Institute of Molecular Medicine, UTHealth-McGovern Medical School, Houston, TX, USA. ³Center for Metabolic and Degenerative Diseases, Institute of Molecular Medicine, UTHealth-McGovern Medical School, 1825 Pressler Street, #407-07, Houston, TX 77030, USA. ⁴Department of Anesthesiology, Houston, TX, USA. ⁵Center for Advanced Cardiopulmonary Therapies and Transplantation at UTHealth/McGovern Medical School, Houston, TX, USA. ⁶Division of Pulmonary, Critical Care and Sleep Medicine, Department of Internal Medicine, McGovern Medical School, University of Texas Health Science Center at Houston, 6431 Fannin Street, Suite 6.214, Houston, TX 77030, USA. ⁷Houston Methodist DeBakey Transplant Center, Houston Methodist Hospital, Houston, TX, USA.

Received: 16 September 2024 Accepted: 11 February 2025

Published online: 27 February 2025

References

- Group WHO EAFc-TW, Sterne JAC, Murthy S, Diaz JV, Slutsky AS, Villar J, Angus DC, Annane D, Azevedo LCP, Berwanger O, et al. Association between administration of systemic corticosteroids and mortality among critically ill patients with COVID-19: a meta-analysis. *JAMA*. 2020;324(13):1330–41.
- Zhao Y, Zhao Z, Wang Y, Zhou Y, Ma Y, Zuo W. Single-cell RNA expression profiling of ACE2, the receptor of SARS-CoV-2. *Am J Respir Crit Care Med*. 2020;202(5):756–9.
- Carsana L, Sonzogni A, Nasr A, Rossi RS, Pellegrinelli A, Zerbi P, Rech R, Colombo R, Antinori S, Corbellino M, et al. Pulmonary post-mortem findings in a series of COVID-19 cases from northern Italy: a two-centre descriptive study. *Lancet Infect Dis*. 2020;20(10):1135–40.
- Mangalmurti N, Hunter CA. Cytokine storms: understanding COVID-19. *Immunity*. 2020;53(1):19–25.
- Wang C, Xie J, Zhao L, Fei X, Zhang H, Tan Y, Nie X, Zhou L, Liu Z, Ren Y, et al. Alveolar macrophage dysfunction and cytokine storm in the pathogenesis of two severe COVID-19 patients. *EBioMedicine*. 2020;57: 102833.
- Jahani M, Dokaneheifard S, Mansouri K. Hypoxia: a key feature of COVID-19 launching activation of HIF-1 and cytokine storm. *J Inflamm (Lond)*. 2020;17:33.
- Zhao Z, Zhao Y, Zhou Y, Wang X, Zhang T, Zuo W. Single-cell analysis identified lung progenitor cells in COVID-19 patients. *Cell Prolif*. 2020;53(12): e12931.
- Jyothula SSK, Peters A, Liang Y, Bi W, Shivshankar P, Yau S, Garcha PS, Yuan X, Akkanti B, Collum S, et al. Fulminant lung fibrosis in

- non-resolvable COVID-19 requiring transplantation. *EBioMedicine*. 2022;86: 104351.
9. Desai N, Neyaz A, Szabolcs A, Shih AR, Chen JH, Thapar V, Nieman LT, Solovyov A, Mehta A, Lieb DJ, et al. Temporal and spatial heterogeneity of host response to SARS-CoV-2 pulmonary infection. *Nat Commun*. 2020;11(1):6319.
 10. Alosaimi B, Mubarak A, Hamed ME, Almutairi AZ, Alrashed AA, AlJuryyan A, Enani M, Alenzi FQ, Alturaiki W. Complement anaphylatoxins and inflammatory cytokines as prognostic markers for COVID-19 severity and in-hospital mortality. *Front Immunol*. 2021;12: 668725.
 11. Carvelli J, Demaria O, Vely F, Batista L, Chouaki Benmansour N, Fares J, Carpentier S, Thibault ML, Morel A, Remark R, et al. Association of COVID-19 inflammation with activation of the C5a–C5aR1 axis. *Nature*. 2020;588(7836):146–50.
 12. Hamed ME, Naeem A, Alkadi H, Alamri AA, AlYami AS, AlJuryyan A, Alturaiki W, Enani M, Al-Shouli ST, Assiri AM, et al. Elevated expression levels of lung complement anaphylatoxin, neutrophil chemoattractant chemokine IL-8, and RANTES in MERS-CoV-infected patients: predictive biomarkers for disease severity and mortality. *J Clin Immunol*. 2021;41(7):1607–20.
 13. Malaquias MAS, Gadotti AC, Motta-Junior JDS, Martins APC, Azevedo MLV, Benevides APK, Cezar-Neto P, PaninidoCarmo LA, Zeni RC, Raboni SM, et al. The role of the lectin pathway of the complement system in SARS-CoV-2 lung injury. *Transl Res*. 2021;231:55–63.
 14. Morgan BP, Marchbank KJ, Longhi MP, Harris CL, Gallimore AM. Complement: central to innate immunity and bridging to adaptive responses. *Immunol Lett*. 2005;97(2):171–9.
 15. Sunyer JO, Boshra H, Lorenzo G, Parra D, Freedman B, Bosch N. Evolution of complement as an effector system in innate and adaptive immunity. *Immunol Res*. 2003;27(2–3):549–64.
 16. Volanakis JE. The role of complement in innate and adaptive immunity. *Curr Top Microbiol Immunol*. 2002;266:41–56.
 17. Ling GS, Crawford G, Buang N, Bartok I, Tian K, Thielens NM, Bally I, Harker JA, Ashton-Rickardt PG, Rutschmann S, et al. C1q restrains autoimmunity and viral infection by regulating CD8(+) T cell metabolism. *Science*. 2018;360(6388):558–63.
 18. Beirag N, Varghese PM, Neto MM, Al Ayian A, Khan HA, Qablan M, Shamji MH, Sim RB, Temperton N, Kishore U. Complement activation-independent attenuation of SARS-CoV-2 infection by C1q and C4b-binding protein. *Viruses*. 2023. <https://doi.org/10.3390/v15061269>.
 19. Haslund-Gourley BS, Woloszczuk K, Hou J, Connors J, Cusimano G, Bell M, Taramangalam B, Fourati S, Mege N, Bernui M, et al. IgM N-glycosylation correlates with COVID-19 severity and rate of complement deposition. *Nat Commun*. 2024;15(1):404.
 20. Okamoto T, Mathai SK, Hennessy CE, Hancock LA, Walts AD, Stefanski AL, Brown KK, Lynch DA, Cosgrove GP, Groshong SD, et al. The relationship between complement C3 expression and the MUC5B genotype in pulmonary fibrosis. *Am J Physiol Lung Cell Mol Physiol*. 2018;315(1):L1–10.
 21. Li H, Tang NL, Chan PK, Wang CY, Hui DS, Luk C, Kwok R, Huang W, Sung JJ, Kong QP, et al. Polymorphisms in the C-type lectin genes cluster in chromosome 19 and predisposition to severe acute respiratory syndrome coronavirus (SARS-CoV) infection. *J Med Genet*. 2008;45(11):752–8.
 22. Ip WK, Chan KH, Law HK, Tso GH, Kong EK, Wong WH, To YF, Yung RW, Chow EY, Au KL, et al. Mannose-binding lectin in severe acute respiratory syndrome coronavirus infection. *J Infect Dis*. 2005;191(10):1697–704.
 23. Zhang H, Zhou G, Zhi L, Yang H, Zhai Y, Dong X, Zhang X, Gao X, Zhu Y, He F. Association between mannose-binding lectin gene polymorphisms and susceptibility to severe acute respiratory syndrome coronavirus infection. *J Infect Dis*. 2005;192(8):1355–61.
 24. Hoffmann D, Mereiter S, Jin OHY, Monteil V, Elder E, Zhu R, Canena D, Hain L, Laurent E, Grunwald-Gruber C, et al. Identification of lectin receptors for conserved SARS-CoV-2 glycosylation sites. *EMBO J*. 2021;40(19): e108375.
 25. Magro C, Mulvey JJ, Berlin D, Nuovo G, Salvatore S, Harp J, Baxter-Stoltzfus A, Laurence J. Complement associated microvascular injury and thrombosis in the pathogenesis of severe COVID-19 infection: A report of five cases. *Transl Res*. 2020;220:1–13.
 26. Gao T, Zhu L, Liu H, Zhang X, Wang T, Fu Y, Li H, Dong Q, Hu Y, Zhang Z, et al. Highly pathogenic coronavirus N protein aggravates inflammation by MASP-2-mediated lectin complement pathway overactivation. *Signal Transduct Target Ther*. 2022;7(1):318.
 27. Kohl J. The role of complement in danger sensing and transmission. *Immunol Res*. 2006;34(2):157–76.
 28. Tschopp J, Chonn A, Hertig S, French LE. Clusterin, the human apolipoprotein and complement inhibitor, binds to complement C7, C8 beta, and the b domain of C9. *J Immunol*. 1993;151(4):2159–65.
 29. Hong SW, Lee J, Kim MJ, Moon SJ, Kwon H, Park SE, Rhee EJ, Lee WY. Clusterin protects lipotoxicity-induced apoptosis via upregulation of autophagy in insulin-secreting cells. *Endocrinol Metab (Seoul)*. 2020;35(4):943–53.
 30. Zhang F, Kumano M, Beraldi E, Fazli L, Du C, Moore S, Sorensen P, Zoubeidi A, Gleave ME. Clusterin facilitates stress-induced lipidation of LC3 and autophagosome biogenesis to enhance cancer cell survival. *Nat Commun*. 2014;5:5775.
 31. Praharaj PP, Patra S, Singh A, Panigrahi DP, Lee HY, Kabir MF, Hossain MK, Patra SK, Patro BS, Patil S, et al. CLU (clusterin) and PPARGC1A/PGC1alpha coordinately control mitophagy and mitochondrial biogenesis for oral cancer cell survival. *Autophagy*. 2024;20(6):1359–82.
 32. Wang C, Yu S, Qian R, Chen S, Dai C, Shan X. Prognostic and immunological significance of peroxisome proliferator-activated receptor gamma in hepatocellular carcinoma based on multiple databases. *Transl Cancer Res*. 2022;11(7):1938–53.
 33. Stoermer KA, Morrison TE. Complement and viral pathogenesis. *Virology*. 2011;411(2):362–73.
 34. Stoiber H, Banki Z, Wilflingseder D, Dierich MP. Complement-HIV interactions during all steps of viral pathogenesis. *Vaccine*. 2008;26(24):3046–54.
 35. Cattaneo R. Four viruses, two bacteria, and one receptor: membrane cofactor protein (CD46) as pathogens' magnet. *J Virol*. 2004;78(9):4385–8.
 36. Jassey A, Jackson WT. Viruses and autophagy: bend, but don't break. *Nat Rev Microbiol*. 2024;22(5):309–21.
 37. Viret C, Rozieres A, Duclaux-Loras R, Boschetti G, Nancey S, Faure M. Regulation of anti-microbial autophagy by factors of the complement system. *Microb Cell*. 2020;7(4):93–105.
 38. Gupta P, Tripathy AS. Alternative pathway of complement activation has a beneficial role against Chandipura virus infection. *Med Microbiol Immunol*. 2020;209(2):109–24.
 39. Suhy DA, Giddings TH Jr, Kirkegaard K. Remodeling the endoplasmic reticulum by poliovirus infection and by individual viral proteins: an autophagy-like origin for virus-induced vesicles. *J Virol*. 2000;74(19):8953–65.
 40. Taylor MP, Kirkegaard K. Modification of cellular autophagy protein LC3 by poliovirus. *J Virol*. 2007;81(22):12543–53.
 41. Garcia-Morales LJ, Chen NY, Weng T, Luo F, Davies J, Philip K, Volcik KA, Melicoff E, Amione-Guerra J, Bunge RR, et al. Altered hypoxic-adenosine axis and metabolism in Group III pulmonary hypertension. *Am J Respir Cell Mol Biol*. 2016;54(4):574–83.
 42. Motulsky HJ, Brown RE. Detecting outliers when fitting data with nonlinear regression - a new method based on robust nonlinear regression and the false discovery rate. *BMC Bioinform*. 2006;7:123.
 43. Sellar GC, Cockburn D, Reid KB. Localization of the gene cluster encoding the A, B, and C chains of human C1q to 1p34.1–1p36.3. *Immunogenetics*. 1992;35(3):214–6.
 44. Kishore U, Reid KB. C1q: structure, function, and receptors. *Immunopharmacology*. 2000;49(1–2):159–70.
 45. Nguyen VC, Tosi M, Gross MS, Cohen-Haguenauer O, Jegou-Foubert C, de Tand MF, Meo T, Frezal J. Assignment of the complement serine protease genes C1r and C1s to chromosome 12 region 12p13. *Hum Genet*. 1988;78(4):363–8.
 46. Falus A, Kramer J, Walcz E, Varga Z, Setalo J, Jobst K, Lakatos T, Meretey K. Unequal expression of complement C4A and C4B genes in rheumatoid synovial cells, human monocytoïd and hepatoma-derived cell lines. *Immunology*. 1989;68(1):133–6.
 47. Zhou Z, Jia D, Kwon O, Li S, Sun H, Roudier MP, Lin DW, True L, Morrissey C, Creighton CJ, et al. Androgen-regulated stromal complement component 7 (C7) suppresses prostate cancer growth. *Oncogene*. 2023;42(32):2428–38.

48. Langeggen H, Pausa M, Johnson E, Casarsa C, Tedesco F. The endothelium is an extrahepatic site of synthesis of the seventh component of the complement system. *Clin Exp Immunol*. 2000;121(1):69–76.
49. Bossi F, Rizzi L, Bulla R, Debeus A, Tripodo C, Picotti P, Betto E, Macor P, Pucillo C, Wurzner R, et al. C7 is expressed on endothelial cells as a trap for the assembling terminal complement complex and may exert anti-inflammatory function. *Blood*. 2009;113(15):3640–8.
50. Choi Y, Bowman JW, Jung JU. Autophagy during viral infection—a double-edged sword. *Nat Rev Microbiol*. 2018;16(6):341–54.
51. Zhang H, Alford T, Liu S, Zhou D, Wang J. Influenza virus causes lung immunopathology through down-regulating PPARgamma activity in macrophages. *Front Immunol*. 2022;13: 958801.
52. Shivshankar P, Li YD, Mueller-Ortiz SL, Wetsel RA. In response to complement anaphylatoxin peptides C3a and C5a, human vascular endothelial cells migrate and mediate the activation of B-cells and polarization of T-cells. *FASEB J*. 2020;34(6):7540–60.
53. Mueller-Ortiz SL, Shivshankar P, Wetsel RA. The second receptor for C5a, C5aR2, is detrimental to mice during systemic infection with listeria monocytogenes. *J Immunol*. 2019;203(10):2701–11.
54. Mueller-Ortiz SL, Calame DG, Shenoi N, Li YD, Wetsel RA. The complement anaphylatoxins C5a and C3a suppress IFN-beta production in response to listeria monocytogenes by inhibition of the cyclic dinucleotide-activated cytosolic surveillance pathway. *J Immunol*. 2017;198(8):3237–44.
55. Deiteren K, Hendriks D, Scharpe S, Lambeir AM. Carboxypeptidase M: multiple alliances and unknown partners. *Clin Chim Acta*. 2009;399(1–2):24–39.
56. Maier T, Guell M, Serrano L. Correlation of mRNA and protein in complex biological samples. *FEBS Lett*. 2009;583(24):3966–73.
57. Koussounadis A, Langdon SP, Um IH, Harrison DJ, Smith VA. Relationship between differentially expressed mRNA and mRNA-protein correlations in a xenograft model system. *Sci Rep*. 2015;5:10775.
58. Wu M, Chen Y, Xia H, Wang C, Tan CY, Cai X, Liu Y, Ji F, Xiong P, Liu R, et al. Transcriptional and proteomic insights into the host response in fatal COVID-19 cases. *Proc Natl Acad Sci U S A*. 2020;117(45):28336–43.
59. Cheng Z, Teo G, Krueger S, Rock TM, Koh HW, Choi H, Vogel C. Differential dynamics of the mammalian mRNA and protein expression response to misfolding stress. *Mol Syst Biol*. 2016;12(1):855.
60. Anderson BD, Nakamura T, Russell SJ, Peng KW. High CD46 receptor density determines preferential killing of tumor cells by oncolytic measles virus. *Cancer Res*. 2004;64(14):4919–26.
61. Garcia-Pardo J, Tanco S, Diaz L, Dasgupta S, Fernandez-Recio J, Lorenzo J, Aviles FX, Fricker LD. Substrate specificity of human metallopeptidase D: comparison of the two active carboxypeptidase domains. *PLoS ONE*. 2017;12(11): e0187778.
62. Hadkar V, Skidgel RA. Carboxypeptidase D is up-regulated in raw 264.7 macrophages and stimulates nitric oxide synthesis by cells in arginine-free medium. *Mol Pharmacol*. 2001;59(5):1324–32.
63. Mevorach D, Mascarenhas JO, Gershov D, Elkon KB. Complement-dependent clearance of apoptotic cells by human macrophages. *J Exp Med*. 1998;188(12):2313–20.
64. Kisserli A, Schneider N, Audonnet S, Tabary T, Goury A, Cousson J, Mahmoudi R, Bani-Sadr F, Kanagaratnam L, Jolly D, et al. Acquired decrease of the C3b/C4b receptor (CR1, CD35) and increased C4d deposits on erythrocytes from ICU COVID-19 patients. *Immunobiology*. 2021;226(3): 152093.
65. Ye J, Yang P, Yang Y, Xia S. Complement C1s as a diagnostic marker and therapeutic target: Progress and prospective. *Front Immunol*. 2022;13:1015128.
66. Peitsch MC, Kovacovics TJ, Tschopp J, Isliker H. Antibody-independent activation of C1. II. Evidence for two classes of nonimmune activators of the classical pathway of complement. *J Immunol*. 1987;138(6):1871–6.
67. Kovacovics TJ, Peitsch MC, Kress A, Isliker H. Antibody-independent activation of C1. I. Differences in the mechanism of C1 activation by nonimmune activators and by immune complexes: C1r-independent activation of C1s by cardiolipin vesicles. *J Immunol*. 1987;138(6):1864–70.
68. McGrath FD, Brouwer MC, Arlaud GJ, Daha MR, Hack CE, Roos A. Evidence that complement protein C1q interacts with C-reactive protein through its globular head region. *J Immunol*. 2006;176(5):2950–7.
69. Brasen CL, Christensen H, Olsen DA, Kahns S, Andersen RF, Madsen JB, Lassen A, Kierkegaard H, Jensen A, Sydenham TV, et al. Daily monitoring of viral load measured as SARS-CoV-2 antigen and RNA in blood, IL-6, CRP and complement C3d predicts outcome in patients hospitalized with COVID-19. *Clin Chem Lab Med*. 2021;59(12):1988–97.
70. Agrati C, Bartolini B, Bordoni V, Locatelli F, Capobianchi MR, Di Caro A, Castilletti C, Ippolito G. Emerging viral infections in immunocompromised patients: a great challenge to better define the role of immune response. *Front Immunol*. 2023;14:1147871.
71. Rossi V, Teillet F, Thielens NM, Bally I, Arlaud GJ. Functional characterization of complement proteases C1s/mannan-binding lectin-associated serine protease-2 (MASP-2) chimeras reveals the higher C4 recognition efficacy of the MASP-2 complement control protein modules. *J Biol Chem*. 2005;280(51):41811–8.
72. Thielens NM, Tacnet-Delorme P, Arlaud GJ. Interaction of C1q and mannan-binding lectin with viruses. *Immunobiology*. 2002;205(4–5):563–74.
73. Gal P, Ambrus G, Zavodszky P. C1s, the protease messenger of C1. Structure, function and physiological significance. *Immunobiology*. 2002;205(45):383–94.
74. Lu J, Kishore U. C1 complex: an adaptable proteolytic module for complement and non-complement functions. *Front Immunol*. 2017;8:592.
75. Degn SE, Jensen L, Olszowski T, Jensenius JC, Thiel S. Co-complexes of MASP-1 and MASP-2 associated with the soluble pattern-recognition molecules drive lectin pathway activation in a manner inhibitable by MAP44. *J Immunol*. 2013;191(3):1334–45.
76. Holers VM, Borodovsky A, Scheinman RI, Ho N, Ramirez JR, Dobo J, Gal P, Lindenberger J, Hansen AG, Desai D, et al. Key components of the complement lectin pathway are not only required for the development of inflammatory arthritis but also regulate the transcription of factor D. *Front Immunol*. 2020;11:201.
77. Gotz MP, Skjoed MO, Bayarri-Olmos R, Hansen CB, Perez-Alos L, Jarlhelt I, Benfield T, Rosbjerg A, Garred P. Lectin pathway enzyme MASP-2 and downstream complement activation in COVID-19. *J Innate Immun*. 2022. <https://doi.org/10.1159/000525508>.
78. Rawal N, Rajagopalan R, Salvi VP. Stringent regulation of complement lectin pathway C3/C5 convertase by C4b-binding protein (C4BP). *Mol Immunol*. 2009;46(15):2902–10.
79. Macsik-Valent B, Nagy K, Fazekas L, Erdei A. Complement receptor type 1 (CR1, CD35), the inhibitor of BCR-mediated human B cell activation, differentially regulates TLR7, and TLR9 induced responses. *Front Immunol*. 2019;10:1493.
80. Kopf M, Abel B, Gallimore A, Carroll M, Bachmann MF. Complement component C3 promotes T-cell priming and lung migration to control acute influenza virus infection. *Nat Med*. 2002;8(4):373–8.
81. Kim YJ, Kim KH, Ko EJ, Kim MC, Lee YN, Jung YJ, Lee YT, Khwon YM, Song JM, Kang SM. Complement C3 plays a key role in inducing humoral and cellular immune responses to influenza virus strain-specific hemagglutinin-based or cross-protective M2 extracellular domain-based vaccination. *J Virol*. 2018. <https://doi.org/10.1128/JVI.00969-18>.
82. Posch W, Vosper J, Noureen A, Zaderer V, Witting C, Bertacchi G, Gstir R, Filipek PA, Bonn GK, Huber LA, et al. C5aR inhibition of nonimmune cells suppresses inflammation and maintains epithelial integrity in SARS-CoV-2-infected primary human airway epithelia. *J Allergy Clin Immunol*. 2021;147(6):2083–20972086.
83. Perl A. mTOR-dependent autophagy contributes to end-organ resistance and serves as target for treatment in autoimmune disease. *EBioMedicine*. 2018;36:12–3.
84. Yang Z, Goronzy JJ, Weyand CM. Autophagy in autoimmune disease. *J Mol Med (Berl)*. 2015;93(7):707–17.
85. Van Grol J, Subauste C, Andrade RM, Fujinaga K, Nelson J, Subauste CS. HIV-1 inhibits autophagy in bystander macrophage/monocytic cells through Src-Akt and STAT3. *PLoS ONE*. 2010;5(7): e11733.
86. Zhou J, Zhang W, Liang B, Casimiro MC, Whitaker-Menezes D, Wang M, Lisanti MP, Lanza-Jacoby S, Pestell RG, Wang C. PPARgamma activation induces autophagy in breast cancer cells. *Int J Biochem Cell Biol*. 2009;41(11):2334–42.
87. Lee MS, Jones T, Song DY, Jang JH, Jung JU, Gao SJ. Exploitation of the complement system by oncogenic Kaposi's sarcoma-associated herpesvirus for cell survival and persistent infection. *PLoS Pathog*. 2014;10(9): e1004412.

88. Weyand NJ, Lee SW, Higashi DL, Cawley D, Yoshihara P, So M. Monoclonal antibody detection of CD46 clustering beneath *Neisseria gonorrhoeae* microcolonies. *Infect Immun*. 2006;74(4):2428–35.
89. Feito MJ, Sanchez A, Oliver MA, Perez-Caballero D, Roriguez de Cordoba S, Alberti S, Rojo JM. Membrane cofactor protein (MCP, CD46) binding to clinical isolates of *Streptococcus pyogenes*: binding to M type 18 strains is independent of Emm or Enn proteins. *Mol Immunol*. 2007;44(14):3571–9.
90. Hemsath JR, Liaci AM, Rubin JD, Parrett BJ, Lu SC, Nguyen TV, Turner MA, Chen CY, Cupelli K, Reddy VS, et al. Ex vivo and in vivo CD46 receptor utilization by species D human adenovirus serotype 26 (HAdV26). *J Virol*. 2022;96(3): e0082621.
91. Gebetsberger L, Malekshahi Z, Teutsch A, Tajti G, Fontaine F, Marella N, Mueller A, Prantl L, Stockinger H, Stoiber H, et al. SARS-CoV-2 hijacks host CD55, CD59 and factor H to impair antibody-dependent complement-mediated lysis. *Emerg Microbes Infect*. 2024;13(1):2417868.
92. Ozen A, Chongsrisawat V, Sefer AP, Kolukisa B, Jalbert JJ, Meagher KA, Brackin T, Feldman HB, Baris S, Karakoc-Aydiner E, et al. Evaluating the efficacy and safety of pozelimab in patients with CD55 deficiency with hyperactivation of complement, angioathic thrombosis, and protein-losing enteropathy disease: an open-label phase 2 and 3 study. *Lancet*. 2024;403(10427):645–56.
93. Ge X, Yu Z, Guo X, Li L, Ye L, Ye M, Yuan J, Zhu C, Hu W, Hou Y. Complement and complement regulatory proteins are upregulated in lungs of COVID-19 patients. *Pathol Res Pract*. 2023;247: 154519.
94. Hourcade DE. The role of properdin in the assembly of the alternative pathway C3 convertases of complement. *J Biol Chem*. 2006;281(4):2128–32.
95. Varghese PM, Mukherjee S, Al-Mohanna FA, Saleh SM, Almajhdi FN, Beirag N, Alkahtani SH, Rajkumari R, Nal Rogier B, Sim RB, et al. Human properdin released by infiltrating neutrophils can modulate influenza A virus infection. *Front Immunol*. 2021;12: 747654.
96. Linton SM, Morgan BP. Properdin deficiency and meningococcal disease—identifying those most at risk. *Clin Exp Immunol*. 1999;118(2):189–91.
97. Ma L, Sahu SK, Cano M, Kuppuswamy V, Bajwa J, McPhatter JN, Pine A, Meizlish ML, Goshua G, Chang CH, et al. Increased complement activation is a distinctive feature of severe SARS-CoV-2 infection. *Sci Immunol*. 2021;6(59):2259.
98. Seya T, Atkinson JP. Functional properties of membrane cofactor protein of complement. *Biochem J*. 1989;264(2):581–8.
99. Murugaiah V, Varghese PM, Beirag N, De Cordova S, Sim RB, Kishore U. Complement proteins as soluble pattern recognition receptors for pathogenic viruses. *Viruses*. 2021. <https://doi.org/10.3390/v13050824>.
100. Lucientes-Continente L, Marquez-Tirado B, Goicoechea de Jorge E. The factor H protein family: the switchers of the complement alternative pathway. *Immunol Rev*. 2023;313(1):25–45.
101. Polycarpou A, Howard M, Farrar CA, Greenlaw R, Fanelli G, Wallis R, Klavinskis LS, Sacks S. Rationale for targeting complement in COVID-19. *EMBO Mol Med*. 2020;12(8): e12642.
102. Vlaar APJ, Witzenzrath M, van Paassen P, Heunks LMA, Mourvillier B, de Bruin S, Lim EHT, Brouwer MC, Tuinman PR, Saraiva JFK, et al. Anti-C5a antibody (vilobelimab) therapy for critically ill, invasively mechanically ventilated patients with COVID-19 (PANAMO): a multicentre, double-blind, randomised, placebo-controlled, phase 3 trial. *Lancet Respir Med*. 2022;10(12):1137–46.
103. Vlaar APJ, de Bruin S, Busch M, Timmermans S, van Zeggeren IE, Koning R, Ter Horst L, Bulle EB, van Baarle F, van de Poll MCG, et al. Anti-C5a antibody IFX-1 (vilobelimab) treatment versus best supportive care for patients with severe COVID-19 (PANAMO): an exploratory, open-label, phase 2 randomised controlled trial. *Lancet Rheumatol*. 2020;2(12):e764–73.
104. Carvelli J, Meziani F, Dellamonica J, Cordier PY, Allardet-Servent J, Fraisse M, Velly L, Barbar SD, Lehighue S, Guervilly C, et al. Avdoralimab (anti-C5aR1 mAb) versus placebo in patients with severe COVID-19: results from a randomized controlled trial (FOR COVID elimination [FORCE]). *Crit Care Med*. 2022;50(12):1788–98.

Publisher's Note

Springer Nature remains neutral with regard to jurisdictional claims in published maps and institutional affiliations.